Thermo-Responsive Injectable Hydrogel System Based on Poly(*N*-isopropylacrylamide-*co*-vinylphosphonic acid). I. Biomineralization and Protein Delivery

So Yeon Kim,[1] Sang Cheon Lee[2]

[1]*Division of Engineering Education, College of Engineering, Chungnam National University, Daejeon 305-764, South Korea*
[2]*Nanomaterials Application Division, Korea Institute of Ceramic Engineering and Technology, Seoul 153-801, South Korea*

Received 6 August 2008; accepted 21 January 2009
DOI 10.1002/app.30318
Published online 8 May 2009 in Wiley InterScience (www.interscience.wiley.com).

ABSTRACT: To achieve the injectable hydrogel system in order to improve bone regeneration by locally delivering a protein drug including bone morphogenetic proteins, thermo-responsive injectable hydrogels composed of *N*-isopropylacrylamide (NIPAAm) and vinyl phosphonic acid (VPAc) were prepared. The P(NIPAAm-*co*-VPAc) hydrogels were also biomineralized by urea-mediation method to create functional polymer hydrogels that deliver the protein drug and mimic the bone extracellular matrix. The loosely cross-linked P(NIPAAm-*co*-VPAc) hydrogels were pliable and fluid-like at room temperature and could be injected through a small-diameter aperture. The lower critical solution temperature (LCST) of P(NIPAAm-*co*-VPAc) hydrogel was influenced by the monomer ratio of NIPAAm/VPAc and the hydrogel with a 96/4 molar ratio of NIPAAm/VPAc exhibited an LCST of ~34.5°C. Water content was influenced by temperature, NIPAAm/VPAc monomer ratio, and biomineralization; however, all hydrogels maintained more than about 77% of the water content even at 37°C. In a cytotoxicity study, the P(NIPAAm-*co*-VPAc) and biomineralized P(NIPAAm-*co*-VPAc) hydrogels did not significantly affect cell viability. The loading content of bovine serum albumin in hydrogel, which was used as a model drug, gradually increased with the amount of VPAc in the hydrogel owing to the ionic interaction between VPAc groups and BSA molecules. In addition, the release behavior of BSA from the P(NIPAAm-*co*-VPAc) hydrogels was mainly influenced by the drug loading content, water content, and biomineralization of the hydrogels. © 2009 Wiley Periodicals, Inc. J Appl Polym Sci 113: 3460–3469, 2009

Key words: hydrogel; protein delivery; mineralization; PNIPAAm; VPAc

INTRODUCTION

Recent advances in biotechnology have resulted in a great variety of pharmaceutically active peptides and proteins. However, therapeutic proteins and peptides administered are often cleared rapidly from circulation and, therefore, need to be administered frequently in order to maintain therapeutic levels in the blood.[1–7] One of the major issues which limit the therapeutic applicability of these protein-based drugs is the lack of suitable dosage forms; thus, a demand for novel methods of delivering these drugs and a necessity for new drug release strategies have arisen.[3–7]

In one of these strategies, hydrogels are considered to be interesting carriers/vessels for peptide and protein delivery because of their good tissue compatibility and the possibilities that allow for manipulation of the permeability for drug molecules.[8–15] Hydrogels are crosslinked hydrophilic polymer networks, and may absorb more than 1000× their dry weight in water, giving them physical characteristics similar to soft tissues. Over the past three decades, chemically and physically diverse hydrogels have become standard materials for drug delivery, contact lenses, corneal implants, and scaffolds for the regeneration of new skin, encapsulation of cells, and the regeneration of tendons and cartilage.[8–15]

In recent years, there has been a growing interest in *in situ* gel-forming systems as candidates for drug and cell delivery.[9,16–21] Several methods have been developed for the preparation of self-gelling hydrogels that are cross-linked by non-permanent bonds based on physical interactions between the polymer chains. Such systems can be administered by injection in liquid form, which then gels *in situ*. The following mechanisms may be involved in the *in situ* gel formation: gelation in response to temperature or pH change, ionic cross-linking, solvent exchange or crystallization, and thickening upon removal of the injection shear. Gel formation through chemical

Correspondence to: S. Y. Kim (kimsy@cnu.ac.kr).

cross-linking can also occur when UV light is used as a trigger.[16]

Several hydrogel systems have been designed through the development of a thermally reversible gelling property for drug delivery systems.[8–16,17,18] After being locally injected to a specific body site, the solution incorporated with physically mixed drugs can be instantly converted to hydrogel at the injected site via hydrophobic interaction between hydrophobic moieties in the polymers. Then, the loaded drugs are slowly released through three-dimensional networks of the hydrogels; such networks have attracted great interest in contemporary drug research because of their simple systemic formulation for drug delivery.[16]

The main objective of this study is to prepare the injectable hydrogel system to improve bone regeneration by locally delivering native or recombinant human BMP. An optimized delivery system might improve the osteopotency of the device while reducing as much as possible the amount of introduced BMP, which offers the double advantage of being safer as well as less expensive.

Natural bone is a composite of collagen, a protein-based hydrogel template, and inorganic dahilite (carbonated apatite) crystals.[22] It was reported that acidic extracellular matrix proteins that are attached to the collagen scaffolds play important templating and inhibitory roles during the mineralization process.[22–25] The acidic groups serve as binding sites for calcium ions and align them in an orientation that matches the apatite crystal lattice.[22,23]

In this study, we focused on the thermo-responsive injectable hydrogels that can be formulated at room temperature and form a gel at body temperature. Poly(*N*-isopropylacrylamide) (PNIPAAm), the most popular thermo-sensitive, water-soluble polymer, exhibits a lower critical solution temperature (LCST) of almost 32°C.[8] PNIPAAm chains hydrate to form an expanded structure at temperatures lower than 32°C, but undergo a sharp phase transition at higher temperatures to form inter- and intrachain associations, resulting in precipitation.[8–15] These types of phase transitions can be exploited to develop injectable liquid materials at room temperature, and form viscoelastic solids at physiological temperature.[16,18,19]

In the present study, we synthesized loosely cross-linked hydrogels composed of thermo-responsive *N*-isopropylacrylamide (NIPAAm) and vinyl phosphonic acid (VPAc) which can serve as binding sites for calcium ions during the mineralization process. Then, the P(NIPAAm-*co*-VPAc) hydrogels were mineralized by urea-mediated method. To evaluate the feasibility of injectable thermo-responsive hydrogels, the LCST and the water content of the P(NIPAAm-*co*-VPAc) and biomineralized P(NIPAAm-*co*-VPAc) hydrogels were characterized. The *in vitro* release behavior of the model protein drug from the P(NIPAAm-*co*-VPAc) hydrogels was also evaluated.

MATERIALS AND METHODS

Materials

N-Isopropylacrylamide (NIPAAm), vinylphosphonic acid (VPAc), poly(ethylene glycol) dimethacrylate, ammonium peroxydisulfate (APS), hydroxyapatite, and *N*,*N*,*N*′,*N*′-tetramethylethylenediamine (TEMED) were purchased from Sigma (St. Louis, MO). Urea and hydrolic acid were obtained from Aldrich (Milwaukee, WI). Dulbecco's phosphate-buffered saline (PBS), Dulbecco's Modified Eagle Medium (DMEM, high glucose, with L-glutamine, with pyridoxine hydrochloride, without sodium pyruvate), and heat-inactivated fetal bovine serum (FBS) were purchased from GIBCO BRL (Grand Island, NY). Bovine serum albumin (BSA) was purchased from Sigma (St. Louis, MO). Distilled and deionized water was prepared using a Milli-Q Plus System (Millipore, Bedford, MA). All other chemicals used were reagent grade and were used as purchased without further purification.

Methods

Synthesis of P(NIPAAm-*co*-VPAc) hydrogels

The loosely cross-linked P(NIPAAm-*co*-VPAc) hydrogels were prepared at room temperature by simultaneous free radical polymerization and cross-linking as shown in Figure 1. The hydrogels were prepared by varying the molar ratio of NIPAAm/VPAc and the amount of cross-linker in the feed. The feed molar ratio of NIPAAm/VPAc was changed in the range of 98/2–90/10. The polymerization formulations of hydrogels are described in Table I.

Dry nitrogen gas was bubbled through a mixture of NIPAAm and VPAc, and PEG dimethacrylate (0.1 mol %) in PBS in a flask for 15 min to remove dissolved oxygen. Following the nitrogen gas purge, 0.88 wt % (based on total monomer) of ammonium peroxysulfate (AP) and 8.0 vol/wt % (based on total monomer) of TEMED was added as the initiator and accelerator, respectively. The mixture was stirred vigorously for 30 s and allowed to polymerize at room temperature for 24 h under regular fluorescent light in a glass vial.

Following the polymerization, the P(NIPAAm-*co*-VPAc) hydrogel was washed three times for 15–20 min each in excess ultrapure water (UPW) to remove compounds that had not reacted. In addition, control P(NIPAAm) hydrogels were synthesized by a

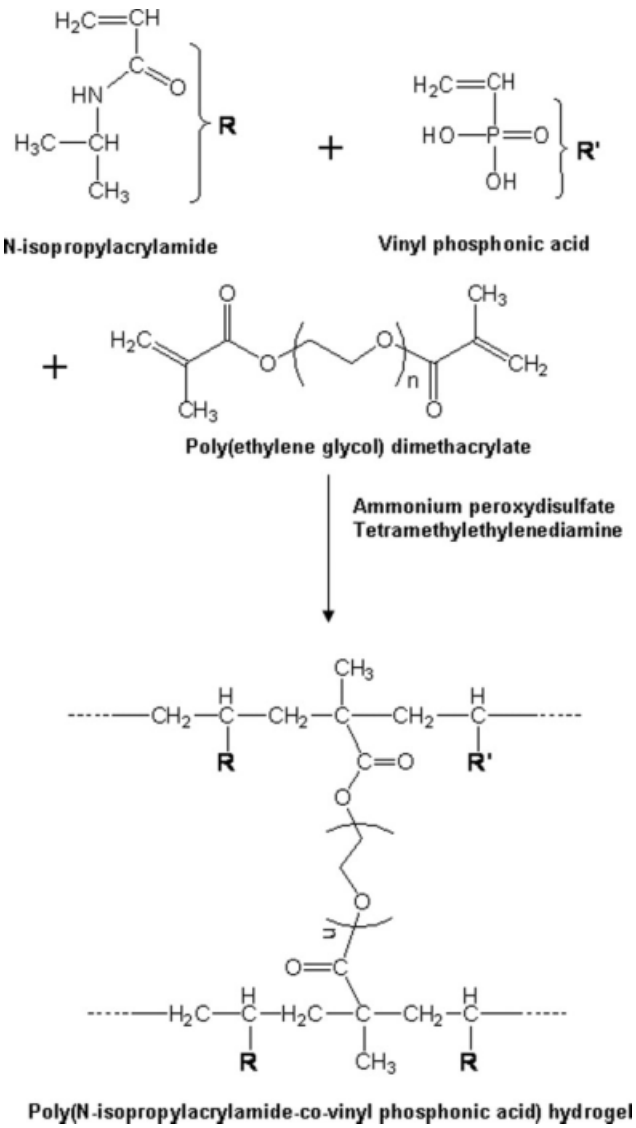

Figure 1 Synthetic scheme of P(NIPAAm-*co*-VPAc) hydrogels.

similar method in order to compare the P(NIPAAm-*co*-VPAc) hydrogels.

Swelling properties of P(NIPAAm-*co*-VPAc) depending on temperature

Forceps were used to carefully grasp a small sample from the top of a P(NIPAAm-*co*-VPAc) hydrogel, and scissors were used to cut samples (about 0.1 g) from the bulk hydrogel. The P(NIPAAm-*co*-VPAc) and P(NIPAAm) hydrogel samples were freeze-dried overnight. The freeze-dried hydrogel samples were weighed upon removal from the freeze-dryer and immersed in excess UPW for 24 h at room temperature and 37°C. The water content was calculated on the basis of the weight difference of the hydrogel samples before and after swelling (water content) $(W_s - W_d)/W_s \times 100$, where W_s is the weight of the swollen gel and W_d is the weight of the dry gel.

To investigate the phase transition of hydrogels depending on temperature, the weight change of hydrogels was also measured as a function of temperature. Hydrogel samples were weighed and immersed in excess UPW in a vial. The temperature was manually ramped at rates of *ca*. 0.1–0.25°C/min for all runs.

Biomineralization of hydrogels

To improve the interaction between hydrogel and osteoblasts, the P(NIPAAm-*co*-VPAc) hydrogels were mineralized by urea-mediated method.[22] Hydroxyapatite (2.92 mmol) was suspended in 100 mL of UPW with stirring, and 2*M* HCl was added sequentially until all the hydroxyapatite suspension was dissolved at a final pH of 2.5–3. Urea (0.2 mol) was then dissolved into the solution to reach a concentration of 2*M*. Each of the hydrogel samples (5.5 cm × 1.5 cm × 1 mm) was then immersed into 50 mL of the acidic HA-urea stock solution. The solution was slowly heated to 90–95°C (within 2 h, with an average heating rate about 0.6°C/min) without agitation of the mineralization solution and maintained at that temperature overnight). The final pH was around 8. Mineralized hydrogel samples were repeatedly washed in UPW to remove loosely attached minerals and soluble ions.

Structural characterization

The structure of the P(NIPAAm-*co*-VPAc) hydrogels was confirmed by FT-IR measurements. FT-IR spectra were recorded on a FT/IR-460 PLUS spectrometer (JASCO, Tokyo, Japan) ranging between 4000 and 650 cm^{-1}, with a resolution of 2 cm^{-1} and 64 scans. The degree of biomineralization of the P(NIPAAm-*co*-VPAc) hydrogel was determined by thermal gravimetric analysis (TGA) using a Metter Toledo TGA/SDTA 851 (Columbus, OH). TGA measurements were performed at temperatures ranging from room temperature to 1100°C at a rate of 5°C/min. P(NIPAAm-*co*-VPAc) hydrogel and biomineralized P(NIPAAm-*co*-VPAc) hydrogels were used for TGA analysis. The degree of biomineralization of hydrogel was determined as weight loss percentage during heating.

In addition, the crystallinity of the materials grown on the surface and inside of the hydrogel was analyzed by X-ray diffraction (XRD). XRD measurements were performed with a Rigaku D/max-RB apparatus (Tokyo, Japan) powder diffractometer and image-plate photography using graphite-monochromatized Cu Kα radiation (λ = 1.542 Å).

TABLE I
Description of P(NIPAAm), P(NIPAAm-*co*-PVAc), and Biomineralized P(NIPAAm-*co*-PVAc) Hydrogels, and Their Water Content and Drug Loading Content

No.	Hydrogel samples	NIPAAm/VPAc monomer ratio in feed[a]	Room temperature[b] (~22°C)	37°C[b]	Drug-loading content (%)[c]
1	P(NIPAAm)	100.0/0.0	98.59 ± 0.16	58.21 ± 1.32	39.98 ± 1.80
2	P(NIPAAm-*co*-VPAc)98/2	98.0/2.0	98.48 ± 0.31	93.91 ± 2.05	49.10 ± 5.08
3	P(NIPAAm-*co*-VPAc)97/3	97.0/3.0	98.43 ± 0.24	94.00 ± 0.93	55.46 ± 1.08
4	P(NIPAAm-*co*-VPAc)96/4	96.0/4.0	98.31 ± 0.11	94.96 ± 1.28	59.44 ± 3.82
5	P(NIPAAm-*co*-VPAc)95/5	95.0/5.0	97.85 ± 0.23	95.75 ± 0.50	63.85 ± 1.80
6	P(NIPAAm-*co*-VPAc)90/10	90.0/10.0	97.74 ± 0.10	96.02 ± 1.14	68.94 ± 2.94
7	B-P(NIPAAm)	100.0/0.0	92.90 ± 0.35	41.94 ± 2.41	22.74 ± 1.32
8	B-P(NIPAAm-*co*-VPAc)98/2[d]	98.0/2.0	92.42 ± 1.42	77.17 ± 1.57	24.24 ± 0.40
9	B-P(NIPAAm-*co*-VPAc)97/3[d]	97.0/3.0	90.99 ± 0.78	79.73 ± 0.58	24.18 ± 1.09
10	B-P(NIPAAm-*co*-VPAc)96/4[d]	96.0/4.0	90.07 ± 1.84	81.68 ± 1.36	21.02 ± 0.45
11	B-P(NIPAAm-*co*-VPAc)95/5[d]	95.0/5.0	89.65 ± 1.44	83.83 ± 1.93	24.67 ± 0.43
12	B-P(NIPAAm-*co*-VPAc)90/10[d]	90.0/10.0	86.87 ± 4.38	84.08 ± 0.91	20.41 ± 1.61

[a] The total amount of NIPAAm and VPAc in feed was always 5 w/v % of reaction media (PBS).
[b] Water content of hydrogel = $(W_s - W_d)/W_s \times 100$, W_s: weight of swollen gel and W_d: weight of dry gel. Each water content value represents the average of four samples.
[c] Drug-loading content (DLC) = (weight of BSA in hydrogel/ weight of dried hydrogel) × 100 = [BSA / (polymer)] × 100.
[d] Biominieralized P(NIPAAm-*co*-PVAc) hydrogel samples.

Data were collected from 20 to 40° in temperature intervals of 0.05° and time intervals of 5 s.

Biocompatibility study

The *in vitro* cytotoxicity of the P(NIPAAm-*co*-VPAc) hydrogels was evaluated using an indirect extraction method.[26,27] Extracts were obtained by immersing fragments of each of the hydrogels (5 cm^2/ mL) in a culture medium at 37°C. After incubation for 5 days, the extracts of the hydrogel samples were collected and diluted to 25, 50, 75, and 100% strength with culture media. Human fibroblast (HF) cells were obtained from the Korea Cell Line Bank. The fibroblasts were incubated using a culture medium composed of DMEM, 10% FBS, and 100 U/mL of penicillin-streptomycin. HF cells were seeded in 96-well plates at a density of 2.0×10^4 cells/well and incubated at 37°C in a wet 5% CO_2 atmosphere for 48 h. After the cells had attached to the wells, the initial culture medium was removed and replaced with the scaffold-extract medium and incubated for 48 h at 37°C. At the end of the incubation period, the extract medium was discarded and the cell viability was determined using the MTT assay ($n = 4$). Fifty microliters of 3-(4, 5-dimethylthiazol-2-yl)-2,5-diphenyl tetrazolium bromide (MTT) solution (12 m*M*) were added to each well. After 4 h of incubation at 37°C, the MTT solution was removed, and the insoluble formazan crystals that formed were dissolved in 150 μL of dimethylsulfoxide (DMSO). The absorbance of the formazan product was measured at 540 nm using a microplate reader (EL310, Bio-Teck Instruments, Winooski, VT). The untreated cells served as a positive control and were taken as being 100% viable.

Protein loading of hydrogels

The model protein used in these experiments was bovine serum (molecular weight = 65,000 Da, Fraction V, Sigma). Solutions of 50.0 mg/mL of BSA were prepared using phosphate buffer. Previously dried hydrogel samples were placed in 20 mL of BSA solution. The sample vials were placed in a temperature-regulated incubator at 4°C. After ~24 h, the samples were taken out of the solution. Then each of the BSA-loaded hydrogels was dried until they obtained a constant weight. The amount of drug loaded into the P(NIPAAm-*co*-VPAc) hydrogel was determined by the weight difference of IPN between the fully swollen state in the aqueous drug solution and the completely dried state.

In vitro release behavior of BSA from P(NIPAAm-*co*-PPAc) hydrogels

Dried BSA-loaded P(NIPAAm-*co*-VPAc) hydrogels were taken and placed in a 25 mL sealed vial containing PBS (0.1*M*, pH 7.4) solution. All release studies were conducted in a shaker agitating at 50 rpm at 37±0.5°C. At predetermined time intervals, 3 mL aliquots of aqueous solution were withdrawn from the release medium and replaced with the same volume of fresh buffer solution. The medium was then analyzed using UV-visible spectrophotometry (Shimadzu Model UV 2101PC, Japan) at 280 nm. The cumulative amount of released BSA was determined

by using the standard calibration curve. All release experiments were carried out in triplicate.

RESULTS AND DISCUSSION

Characterization of P(NIPAAm-*co*-VPAc) hydrogels

To prepare a thermo-responsive injectable hydrogels drug carrier, the P(NIPAAm-*co*-VPAc) hydrogels were prepared by varying the molar ratio of NIPAAm/VPAc in the feed as shown in Table I. FT-IR spectroscopy measurements were carried out to confirm the synthesis of the P(NIPAAm-*co*-VPAc) hydrogels. Figure 2 shows the FT-IR spectra of (a) P(NIPAam-*co*-VPAc)95/5, (b) P(NIPAam-*co*-VPAc)96/4, (c) P(NIPAam-*co*-VPAc)97/3, and (d) P(NIPAAm) hydrogels.

P(NIPAAm) hydrogels show characteristic peaks at 1654, 1542, and 1375 cm^{-1}, which can be attributed to the characteristic peaks of amide I, amide II, and a methyl group in $CH(CH_3)_2$, respectively [Fig. 2(d)]. Characteristic peaks of NIPAAm monomer at 1617 cm^{-1} (C=C) and 1410 cm^{-1} (CH_2=) disappeared. In general, the spectrum of P(NIPAAm-*co*-VPAc) including both the characteristic absorptions of NIPAAm and phosphonic acid clearly indicated the presence of amino groups around 3500–3200 cm^{-1} (the stretching of —N—H from PNIPAAm), the ethylene on the polymer backbone at ~2876 cm^{-1}, ~2931 cm^{-1}, ~2968 cm^{-1} (stretching vibrations) as well as 1372–1170 cm^{-1} (twisting and wagging vibrations), the amide I band at ~1636 cm^{-1} (C=O stretching) and amide II band at ~ 1535 cm^{-1} (N—H bending) of the amide group of PNIPAAm. In addition to the peaks mentioned above, the spectrum also contained absorption bands of the asymmetric stretching vibration of the P—O—H group at 1070 cm^{-1}.

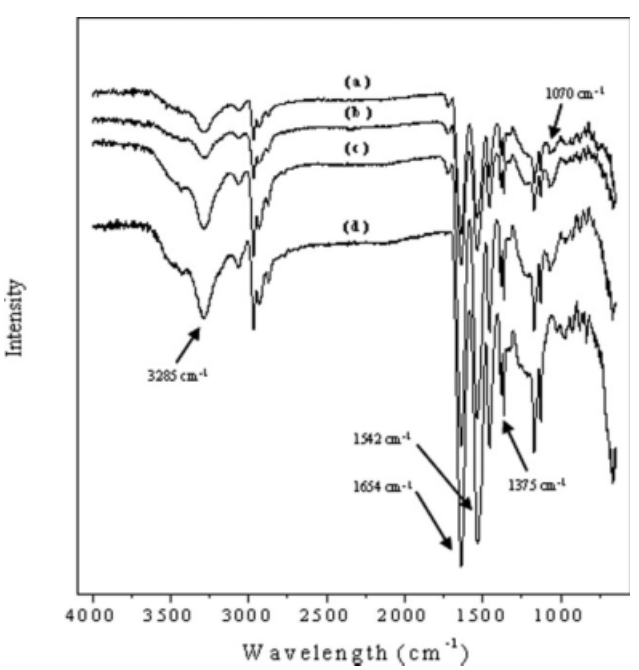

Figure 2 FT-IR spectra of (a) P(NIPAAm-*co*-VPAc)95/5, (b) P(NIPAAm-*co*-VPAc)96/4, (c) P(NIPAAm-*co*-VPAc)97/3, and (d) P(NIPAAm).

As shown in Figure 3, the P(NIPAAm-*co*-VPAc) hydrogel was transparent and exhibited extremely soft and liquid-like characteristics at room temperature (22°C). When the temperature was increased from 22 to 37°C, the P(NIPAAm-*co*-VPAc) hydrogel became a more opaque and rigid structure from the increasing hydrophobic properties of P(NIPAAm) above the LCST. Furthermore, all hydrogels were injectable through a syringe needle aperture without demonstrating appreciable macroscopic fracture at room temperature [Fig. 3(d)]. These results suggest that the *in situ* stabilization of the loosely crosslinked P(NIPAAm-*co*-VPAc) hydrogels at body temperature (37°C) may better support controlled release of protein drugs.

Water content of P(NIPAAm-*co*-VPAc) hydrogels depending on temperature

To estimate the phase transition of hydrogels depending on temperature, the weight change of the hydrogels was also investigated as a function of temperature. Figure 4 shows the swelling profiles of the P(NIPAAm) and P(NIPAAm-*co*-VPAc) hydrogels as a function of temperature. Each line represents a single experiment with one hydrogel sample.

As the temperature increased, the water content of the P(NIPAAm) hydrogels gradually increased and then showed a sharp decrease in water content at ~32°C [Fig. 4(a)] due to the increase in hydrophobic properties of P(NIPAAm) above the LCST. For the P(NIPAAm-*co*-VPAc) hydrogels, the water content increased until ~ 34.5°C and then decreased as shown in Figure 4(b). In general, the addition of more hydrophilic monomers to a P(NIPAAm) hydrogel increases the LCST because the monomer hinders the dehydration of the polymer chains and acts to expand the collapsed structure.[11,13,18,19,28] This indicates that the hydrophilic monomer VPAc influenced changes in the hydrophilic/hydrophobic nature of the polymer, where the incorporation of hydrophilic monomer to the P(NIPAAm) hydrogels increased the LCST value. In addition to an elevated LCST, the P(NIPAAm-*co*-VPAc) hydrogel exhibited a broader transition than the P(NIPAAm) hydrogel, indicating decreased swelling thermosensitivity (i.e. the degree of swelling change with external temperature change). Copolymer hydrogels composed of NIPAAm and a more hydrophilic monomer have demonstrated decreased swelling thermosensitivity

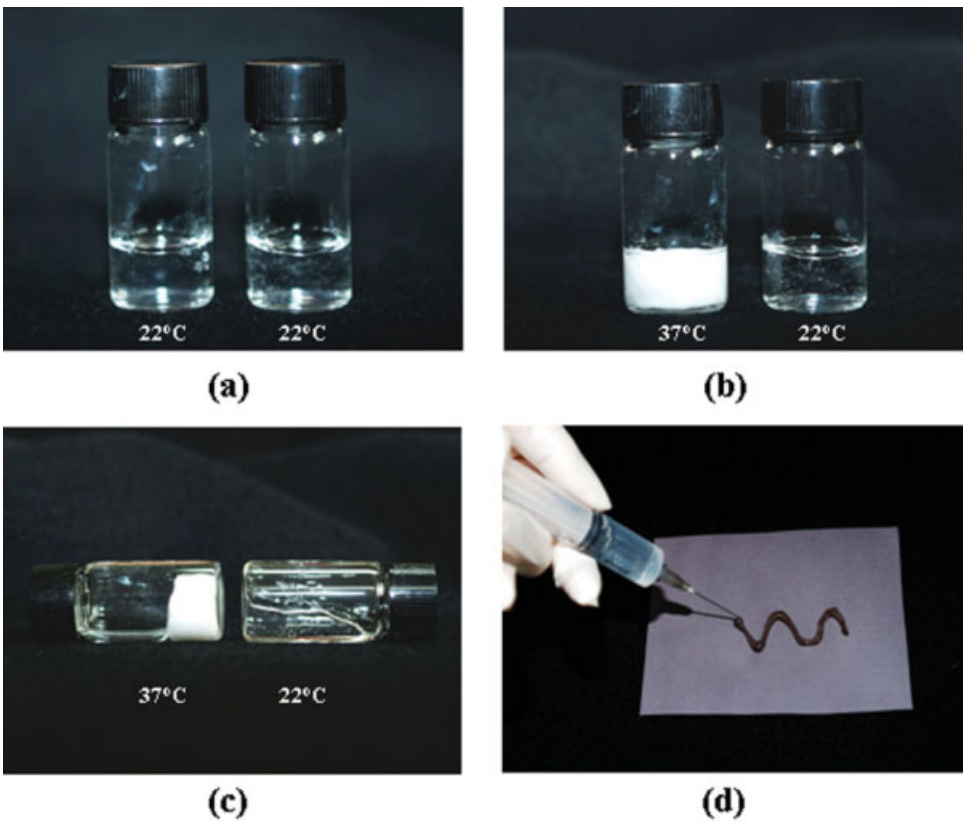

Figure 3 Injectable P(NIPAAm-*co*-VPAc) hydrogels depending on temperature; (a) P(NIPAAm-*co*-VPAc)96/4 hydrogel at 22°C, (b) P(NIPAAm-*co*-VPAc)96/4 hydrogel at 37°C and 22°C, (c) P(NIPAAm-*co*-VPAc)96/4 hydrogel at 37°C and 22°C, and (d) Injectability of P(NIPAAm-*co*-VPAc)96/4 at room temperature. [Color figure can be viewed in the online issue, which is available at www.interscience.wiley.com.]

because the monomer prevents the formation of a compact shrunken structure.

Table I exhibits the water content of the P(NIPAAm) and P(NIPAAm-*co*-VPAc) hydrogels in deionized water at room temperature and 37°C, respectively. At room temperature, all of the P(NIPAAm) and P(NIPAAm-*co*-VPAc) hydrogel samples exhibited water contents of $> 95\%$. As the content of VPAc increased, the water content of the P(NIPAAm-*co*-VPAc) hydrogels gradually decreased at room temperature. It can be estimated that hydrophilic monomer VPAc did not significantly increase the water content of the hydrogel since the phosphonic acid groups did not fully ionize in the swelling medium (deionized water, pH $\sim$ 5.8). Phosphonic acid groups in P(NIPAAm-*co*-VPAc) copolymer dissociate to monobasic and dibasic species around the pH values of 3.1 (pK_1) and 9.0 (pK_2).

The water content of the P(NIPAAm) hydrogels at 37°C significantly decreased until about 58.2%. With the addition of VPAc to the hydrogel, water contents of $> 90\%$ were achieved, even when the temperature was above LCST.

Unlike the swelling properties at room temperature, the water content of the P(NIPAAm-*co*-VPAc) hydrogels at 37°C gradually increased with the VPAc content in hydrogel. It suggests that hydrophilic VPAc prevents the dehydration of the P(NIPAAm-*co*-VPAc) polymer chains and acts to expand the collapsed structure above LCST. This non-shrinking property of the P(NIPAAm-*co*-VPAc) hydrogels at body temperature could be useful for controlled drug delivery.

Biomineralization of P(NIPAAm-*co*-VPAc) hydrogels

P(NIPAAm-*co*-VPAc) hydrogels were biomineralized by urea-mediated method to create functional polymer hydrogels that deliver protein drug and mimic the bone extracellular matrix. After biomineralization, the physical appearance of the P(NIPAAm-*co*-VPAc) hydrogels turned from transparent to white.

In addition, we compared the FT-IR spectra of the non-treated P(NIPAAm-*co*-VPAc) hydrogel [P(NIPAAm-*co*-VPAc)96/4] and the biomineralized hydrogel [B-P(NIPAAm-*co*-VPAc)96/4] as shown in Figure 5(a). The presence of phosphate groups both in the hydroxyapatite and the P(NIPAAm-*co*-VPAc) copolymer complicates the characterization of the

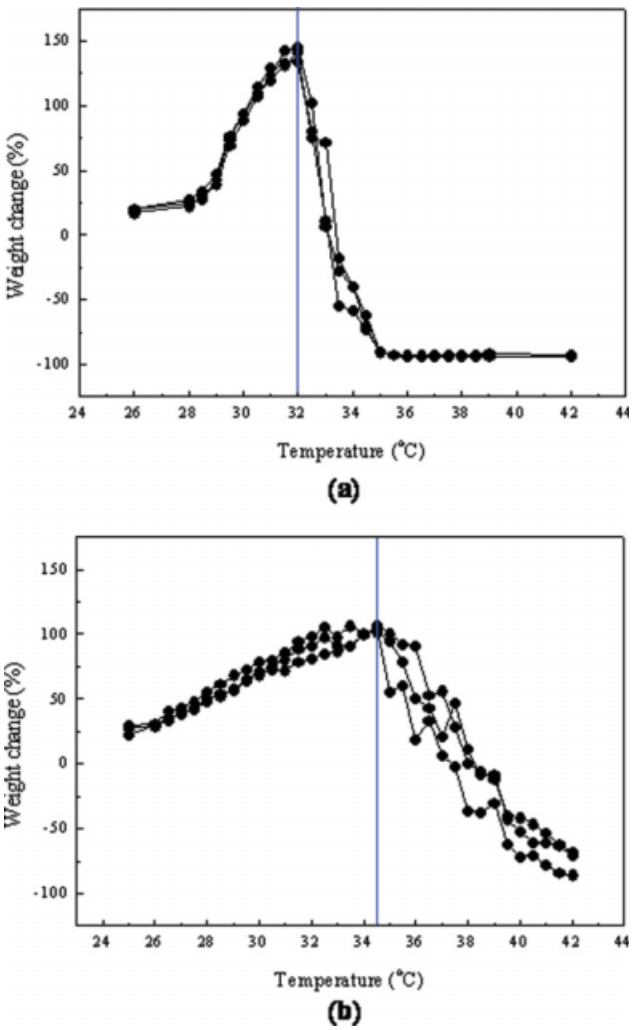

Figure 4 Swelling profiles of P(NIPAAm) and P(NIPAAm-*co*-VPAc) hydrogels depending on temperature, (a) P(NIPAAm), and (b) P(NIPAAm-*co*-VPAc)96/4. Each line represents a single experiment with one hydrogel sample. [Color figure can be viewed in the online issue, which is available at www.interscience.wiley.com.]

apatite growth obtained in the hydrogel samples because its bands overlap with the phosphate groups of the copolymer. After biomineralization, a strong band appeared at 1098 cm^{-1}. This has been attributed to the presence of phosphate salt, indicating the interaction involves the bonding of Ca ions with the P—O^- and $P-O_4^{3-}$ ions of the copolymer ((2) in Figure 5(a)).

In addition, the band at 905 cm^{-1} (assigned to the symmetric vibration of P—O), the band at 970 cm^{-1} (assigned to the asymmetric vibration of P—O), and the band at 1196 cm^{-1} (assigned to the phosphonyl group (P=O) were observed. The FT-IR spectrum also shows the characteristic peaks at 810 cm^{-1} and 684 cm^{-1} which were derived from the hydroxyapatite. These results exhibit the presence of hydroxyapatite in the P(NIPAAm-*co*-PVAc) hydrogel.

The results of XRD analysis for untreated P(NIPAAm-*co*-VPAc) and biomineralized P(NIPAAm-*co*-VPAc) samples are shown in Figure 5(b). The powder XRD patterns obtained from the analysis of the X-ray amorphous copolymers after mineral deposition ((1) and (2) of Figure 5(b)) showed that the prepared P(NIPAAm-*co*-VPAc) hydrogel samples can be identified as a low crystalline apatite. The characteristic diffraction peaks of hydroxyapatite corresponding to the 002, 211, and 300 reflections can be distinguished in the XRD pattern of the biomineralized P(NIPAAm-*co*-VPAc) materials. The characteristic peaks at 2θ regions of 25°, 29°, 30–35°, and 37° indicated the crystalline nature of hydroxyapatite.

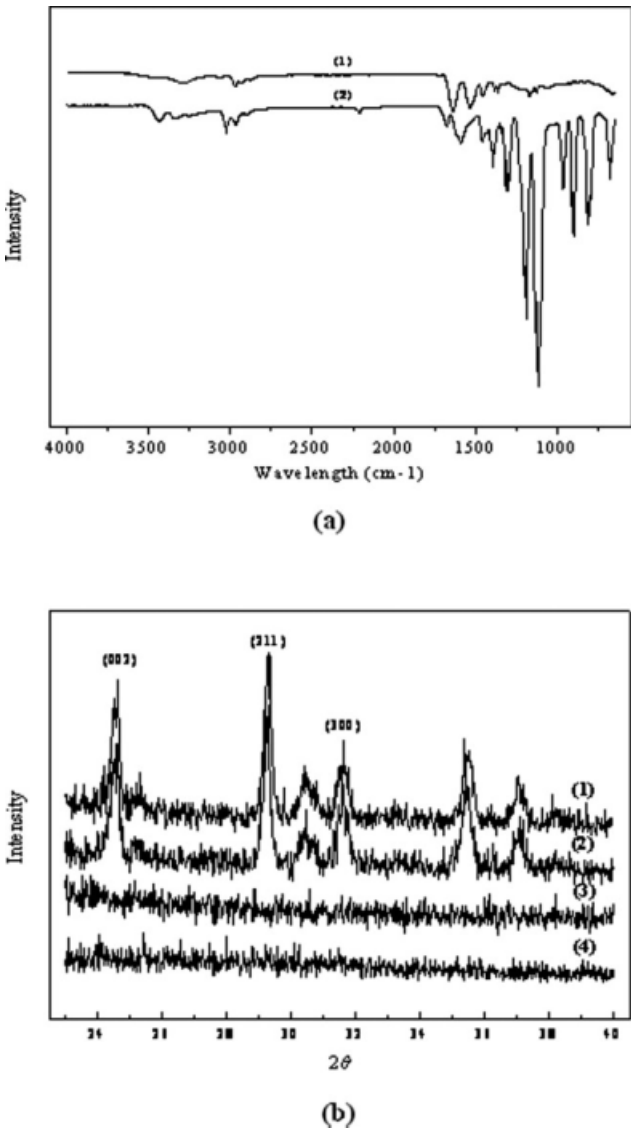

Figure 5 (a) FT-IR spectra of (1) P(NIPAAm-*co*-VPAc)96/4 hydrogel and (2) B-P(NIPAam-*co*-VPAc)96/4 hydrogel; (b) XRD patterns of (1) B-P(NIPAAm-*co*-VPAc)98/2, (2) B-P(NIPAAm-*co*-VPAc)96/4, (3) P(NIPAAm-*co*-VPAc)98/2, and (4) P(NIPAAm-*co*-VPAc)96/4.

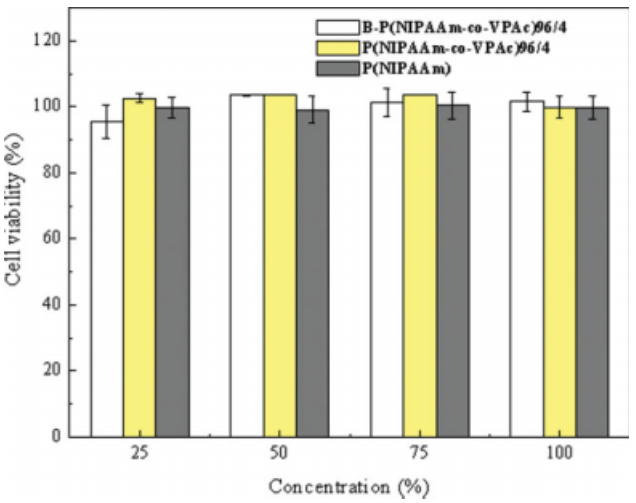

Figure 6 The viability of HFs cultured with extracts of the hydrogels for 48 h, as determined by MTT assay. The viability is expressed as a percentage of the live cells in the samples ($n = 4$) to positive control of cells grown on tissue culture plates lacking any hydrogel material. [Color figure can be viewed in the online issue, which is available at www.interscience.wiley.com.]

To obtain the quantitative data on biomineralization of P(NIPAAm-*co*-VPAc), TGA analysis was performed using dried biomineralized P(NIPAAm-*co*-VPAc) samples. Hydrogel samples were completely dried for 48 h and underwent weight loss less than 1 wt % up to 1100°C; such weight loss is exclusively ascribed to the organic substances and the P(NIPAAm-*co*-VPAc) copolymer. The weight (%) of the residue, and the inorganic component in P(NIPAAm-*co*-VPAc), gradually increased by increasing the content of VPAc in the hydrogels [P(NIPAAm) = 4.57 %; P(NIPAAm-*co*-VPAc)98/2 = 8.71%; P(NIPAAm-*co*-VPAc)96/4 = 11.52%; P(NIPAAm-*co*-VPAc)95/5 = 18.48%]. This indicated that the increase of VPAc content in the P(NIPAAm-*co*-VPAc) hydrogel enhanced intermolecular chelating with calcium ions,[23,24] leading to an increase in nucleation and growth of calcium phosphate in the P(NIPAAm-*co*-VPAc) hydrogel.

Cytotoxicity of P(NIPAAm-*co*-VPAc) hydrogels

The *in vitro* cytotoxicity of P(NIPAAm-*co*-VPAc) hydrogels was investigated using HF by MTT assay, which relies on the mitochondrial activity of vital cells and represents a parameter for their metabolic activity.[24,25] Figure 6 shows the viability of fibroblasts cultured with extracts of the P(NIPAAm), P(NIPAAm-*co*-VPAc), and biomineralized P(NIPAAm-*co*-VPAc) hydrogels. All scaffolds tested showed relatively high cell viability. The viabilities of the fibroblasts were more than 95% within the 48-h observation period. In addition, cell viability was not significantly influenced by the concentration of hydrogel extracts as shown in Figure 6.

Drug loading of P(NIPAAm-*co*-VPAc) hydrogels

Table I exhibits the loading content (%) of BSA in the P(NIPAAm), P(NIPAAm-*co*-VPAc), and biomineralized P(NIPAAm-*co*-VPAc) hydrogels with various compositions. The P(NIPAAm) hydrogels showed about 49.98(%) of DLC, while the DLC of P(NIPAAm-*co*-VPAc) hydrogels gradually increased with the amount of VPAc in the hydrogel [P(NIPAAm-*co*-VPAc)98/2 = 49.10 ± 5.08; P(NIPAAm-*co*-VPAc)97/3 = 55.46 ± 1.08; P(NIPAAm-*co*-VPAc)96/4 = 59.44 ± 3.82; P(NIPAAm-*co*-VPAc)95/5 = 63.85 ± 1.80; P(NIPAAm-*co*-VPAc)90/10 = 68.94 ± 2.94]. This indicated that the ionic interaction between VPAc groups and BSA molecules increased when the amount of ionic VPAc in the hydrogels increased, resulting in an increase in the BSA loading content (%).

For the biomineralized hydrogels, the BSA loading content was lower than the untreated P(NIPAAm-*co*-VPAc) hydrogels (Table I). This result may be due to the decrease in the water content of the hydrogels after biomineralization. In addition, unlike the untreated P(NIPAAm-*co*-VPAc) hydrogels, the amount of ionic VPAc groups in the biomineralized P(NIPAAm-*co*-VPAc) hydrogel did not influence the BSA loading content (%). This suggested that the nucleation and growth of calcium phosphate in hydrogels by biomineralization inhibits an interaction between free VPAc groups and BSA, leading to a decrease in the amount of VPAc on the DLC.

Drug release study

The *in vitro* release kinetics of the model protein BSA from the hydrogels was studied for 9 days. P(NIPAAm-*co*-VPAc) hydrogels with cross-linked network structure was still a coherent mass and could be physically manipulated during release study. The release profiles of BSA from the non-biomineralized hydrogels, shown in Figure 7(a), exhibited sustained release behavior and were influenced by the monomer composition of the hydrogels. The release of BSA became gradually faster [P(NIPAAm) < P(NIPAAm-*co*-VPAc)97/3 < P(NIPAAm-*co*-VPAc)95/5] as the water content and drug release amount of hydrogels increased [P(NIPAAm) = 58.21 ± 1.32(%) water content, 39.98 ± 1.80(%) DLC; P(NIPAAm-*co*-VPAc)97/3 = 94.00 ± 0.93(%) water content, 55.46 ± 1.08(%) DLC; P(NIPAAm-*co*-VPAc)95/5 = 95.75 ± 0.50(%) water content, 63.85 ± 1.80(%) DLC]. This result was attributed to the increasing driving forces, i.e. the concentration difference and swelling of the hydrogels, for drug diffusion.

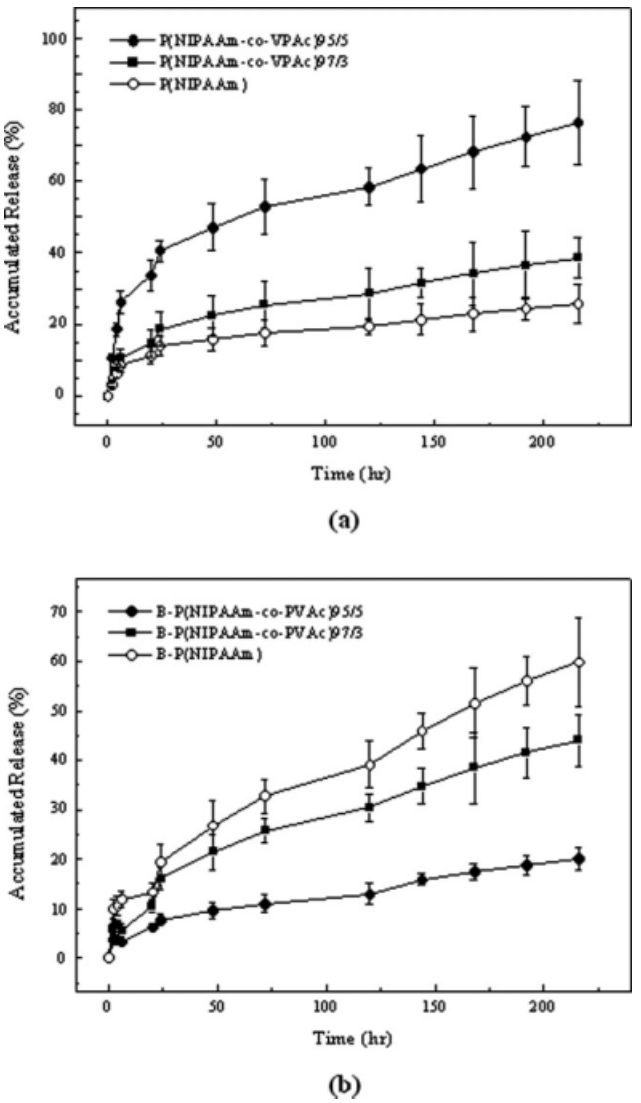

Figure 7 *In vitro* release kinetics of BSA from hydrogels at 37°C; (a) Release behavior of BSA from P(NIPAAm-*co*-VPAc)95/5, P(NIPAAm-*co*-VPAc)97/3, and P(NIPAAm), (b) Release behavior of BSA from B-P(NIPAAm-*co*-VPAc)95/5, B-P(NIPAAm-*co*-VPAc)97/3, and B-P(NIPAAm). Each point represents the mean ± SD of three samples.

Unlike the non-biomineralized hydrogels, the release kinetics of BSA from the biomineralized hydrogels, which had a similar DLC regardless of the hydrogel composition [B-P(NIPAAm) = 32.74 ± 1.32 (%); B-P(NPAAm-*co*-VPAc)97/3 = 34.18 ± 1.09 (%); B-P(NIPAAm-*co*-VPAc) = 34.67 ± 0.43 (%), as shown in Table I], showed opposite tendencies [Fig. 7(b)]. The release behavior of BSA became gradually slower [P(NIPAAm) > P(NIPAAm-*co*-VPAc)97/3 > P(NIPAAm-*co*-VPAc)95/5] when the VPAc ionic groups in hydrogels increased in spite of the increase in water content. This indicated that the release behavior of BSA from the biomineralized hydrogels with similar DLC and relative low water content (compared with the non-biomineralized hydrogels) was mainly influenced by the interaction between ionic groups in the hydrogel and protein drug molecules.

CONCLUSIONS

Thermo-responsive and injectable P(NIPAAm-*co*-VPAc) hydrogels were prepared as a local protein drug delivery system for bone and cartilage regeneration. To mimic bone extracellular matrix, the organic/inorganic hybrid P(NIPAAm-*co*-VPAc) hydrogels were developed through a biomineralization process. The increase of VPAc groups in the hydrogels enhanced an intermolecular chelating with calcium ions, leading to a increase in nucleation and growth of calcium phosphate in the hydrogels. The P(NIPAAm-*co*-VPAc) hydrogels showed liquid-like properties and injectability through a small-diameter aperture at room temperature. The LCST of the P(NIPAAm-*co*-VPAc) hydrogel was influenced by the addition of VPAc and the hydrogel with 96/4 molar ratio of NIPAAm/VPAc exhibited an LCST of ~34.5°C. The P(NIPAAm-*co*-VPAc) hydrogels maintained more than about 77% of water content even at 37°C (above the LCST). The P(NIPAAm-*co*-VPAc) and biomineralized P(NIPAAm-*co*-VPAc) hydrogels did not significantly affect cell viability in the cytotoxicity study. The BSA loading content in the hydrogel gradually increased with the amount of VPAc in the hydrogel. The release kinetics of BSA of the hydrogels was dependent upon the DLC, water content, and biomineralization of the hydrogels. These results suggest that P(NIPAAm-*co*-VPAc) and biomineralized P(NIPAAm-*co*-VPAc) hydrogels can be tailored to create an injectable hydrogel system for controlled protein delivery.

This study was financially supported by research fund of Chungnam National University in 2007

References

1. Ginty, P. J.; Barry, J. J. A.; White, L. J.; Howdle, S. M.; Shakesheff, K. M. Eur J Pharm Biopharm 2008, 68, 82.
2. Hennink, W. E.; Talsma, H.; Borchert, J. C. H.; De Smedt, S. C.; Demeester, J. J Controlled Release 1996, 39, 47.
3. Gayet, J. C.; Fortier, G. J Controlled Release 1996, 38, 177.
4. Lin, Y. H.; Liang, H. F.; Chung, C. K.; Chen, M. C.; Sung, H. W. Biomaterials 2005, 26, 2105.
5. Dorkoosh, F. A.; Verhoef, J. C.; Ambagts, M. H. C.; Rafiee-Tehrani, M.; Borchard, G.; Junginger, H. E. Eur J Pharm Sci 2002, 15, 433.
6. Maire, M.; Chaubet, F.; Mary, P.; Blanchat, C.; Meunier, A.; Logeart-Avramoglou, D. Biomaterials 2005, 26, 5085.
7. Gumusderelioglu, M.; Kesgin, D. Int J Pharm 2005, 288, 273.
8. Rzaev, Z. M. O.; Dincer, S.; Piskin, E. Prog Polym Sci 2007, 32, 534.
9. Tang, Y. F.; Du, Y. M.; Hu, X. W.; Shi, X. W.; Kennedy, J. F. Carbohydr Polym 2007, 67, 491.

10. Abd El-Mohdy, H. L.; Safrany, A. Radiat Phys Chem 2008, 77, 273.
11. Mohan, Y. M.; Premkumar, T.; Joseph, D. K.; Geckeler, K. E. React Functional Polym 2007, 67, 844.
12. Wu, J.-Y.; Liu, S.-Q.; Heng, P. W.-S.; Yang, Y.-Y. J Controlled Release 2005, 102, 361.
13. Wang, L.-P.; Wang, Y.-P.; Pei, X.-W.; Peng, B. React Functional Polym 2008, 68, 649.
14. Li, X.; Wu, W.; Liu, W. Carbohydr Polym 2008, 71, 394.
15. Uludag, H.; Norrie, B.; Kousinioris, N.; Gao, T. Biotechnol Bioeng 2001, 73, 510.
16. Gutowska, A.; Jeong, B.; Jasionowski, M. The Anatomical Record 2001, 263, 342.
17. Burdick, J. A.; Anseth, K. S. Biomaterials 2002, 23, 4315.
18. Kim, S. Y.; Healy, K. E. Biomacromolecules 2003, 4, 1214.
19. Kim, S. Y.; Chung, E. H.; Gilbert, M.; Healy, K. E. J Biomed Mater Res 2005, 75, 73.
20. Trojani, C.; Weiss, P.; Michiels, J.-F.; Vinatier, C.; Guicheux, J.; Daculsi, G.; Gaudray, P.; Carle, G. F.; Rochet, N. Biomaterials 2005, 26, 5509.
21. Shu, X. Z.; Liu, Y.; Palumbo, F. S.; Luo, Y.; Prestwich, G. D. Biomaterials 2004, 25, 1339.
22. Song, J.; Saiz, E.; Bertozzi, C. R. J Eur Ceram Soc 2003, 23, 2905.
23. Dogan, O.; Oner, M. Langmuir 2006, 22, 9671.
24. Nuttelman, C. R.; Benoit, D. S. W.; Tripodi, M. C.; Anseth, K. S. Biomaterials 2006, 27, 1377.
25. Al-Ali, F.; Lebugle, A.; Rico-Lattes, L.; Etemad-Moghadam, G. J Colloid Interface Sci 2005, 289, 504.
26. Pariente, J.-L.; Kim, B.-S.; Atala, A. J Biomed Mater Res 2001, 55, 33.
27. Zange, R.; Li, Y.; Kissel, T. J Controlled Release 1998, 56, 249.
28. Kurkuki, M. D.; Nussio, M. R.; Deslandes, A.; Voelcker, N. H. Langmuir 2008, 24, 4238.